

# Strongly bound mesons at finite temperature and in magnetic fields from AdS/CFT

---

K. D. Jensen, A. Karch, J. Price

*Department of Physics, University of Washington, Seattle, WA 98195-1560*  
kristanj@u.washington.edu, karch@phys.washington.edu;  
cfgauss@u.washington.edu

ABSTRACT: We study mesons in  $\mathcal{N} = 4$  super Yang-Mills theory with fundamental flavors added at large 't Hooft coupling using the gauge/gravity correspondence. High-spin mesons are well described by using semiclassical string configurations. We determine the meson spectrum at finite temperature and in a background magnetic field.

KEYWORDS: AdS/CFT correspondence, thermal field theory.

---

## Contents

<b>1. Introduction</b>	<b>1</b>
<b>2. Meson properties at zero temperature</b>	<b>3</b>
<b>3. Meson dissociation at finite temperature</b>	<b>5</b>
<b>4. Zeeman effect</b>	<b>6</b>
4.1 General Considerations	6
4.2 Supergravity analysis	9
4.3 $J \ll \sqrt{\lambda}$ , equal charges	12
4.4 $J \ll \sqrt{\lambda}$ , opposite charges	13
<b>5. Meson dissociation in the presence of magnetic fields</b>	<b>13</b>

---

## 1. Introduction

The determination of the bound state spectrum in a Coulomb potential is one of the oldest and most important successes of quantum mechanics. Since the fine-structure constant in nature is small the binding energy is small,  $E_{bind} \sim \alpha^2 m \ll m$ . The bound states are essentially non-relativistic. It is interesting to understand what the properties of bound states look like in the opposite limit of extremely strong Coulomb interactions. One system that realizes such strongly coupled Coulombic bound states is  $\mathcal{N} = 4$  supersymmetric Yang-Mills theory with  $\mathcal{N} = 2$  supersymmetric flavors in the limit of large number of colors  $N_c$  and large 't Hooft coupling. The  $\mathcal{N} = 4$  theory is conformal, which guarantees that the potential between external test particles is of the form  $V(r) = -\frac{c_1}{r}$ . In the large  $N_c$ , large 't Hooft coupling limit the theory can be solved using the AdS/CFT correspondence [1–3]. In particular the coefficient  $c_1$  in the Coulomb potential between external test sources has been determined<sup>1</sup> to be

$$c_1 = \frac{4\pi^2}{\Gamma(\frac{1}{4})^4} \sqrt{\lambda} \tag{1.1}$$

from a Wilson line computation [4, 5].

To realize Coulombic bound states, one needs to add  $N_f$  flavors of dynamical fundamental matter (quarks) to the  $\mathcal{N} = 4$  theory. In the large  $N_c$ , finite  $N_f$  limit this can be achieved via adding flavor probe branes on the supergravity side [6]. In this case conformal invariance

---

<sup>1</sup>We are using conventions where  $\lambda = 2g_{YM}^2 N = 4\pi g_s N$ .

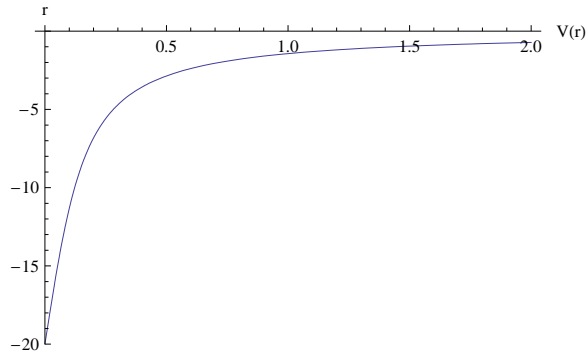


**Figure 1:** Quark/antiquark potential  $V(r)$  in units where the quark mass is  $m = \frac{\sqrt{\lambda}}{2\pi} 10$ .

alone doesn't completely fix the form of the potential. The quantum corrected Coulomb potential instead has the form

$$V(r) = -\frac{c_1}{r} f(mr).$$

where  $m$  denotes the mass of the fundamental flavors. At strong coupling, the function  $f$  can be determined from a static semiclassical string calculation in the bulk. This was first done in [7]. The resulting potential is depicted in figure (1). At large separation (alternatively, at large mass) we need to recover the result for infinitely heavy test quarks and hence  $f \rightarrow 1$ . At small separation,  $f \sim m^2 r^2$  so that the potential becomes linear in distance,  $V(r) = \tau_{eff} r$  with

$$\tau_{eff} = m^2 \frac{2\pi}{\sqrt{\lambda}}. \quad (1.2)$$

The system is highly relativistic in this regime: the glue forms flux tubes that are well described by a relativistic string.

At parametrically small separations,  $mr \sim \frac{1}{\sqrt{\lambda}}$  the determination of  $f$  in terms of a semiclassical string breaks down. To ensure that the mesons we study are insensitive to the details of the potential in this ultra-short distance regime we study mesons with large angular momentum,  $J \gg 1$ . For  $J \gg \sqrt{\lambda}$  the quark/antiquark separation is in the Coulombic regime and the corresponding mesons reproduce hydrogen-like behavior. For  $1 \ll J \ll \sqrt{\lambda}$  the mesons are dominated by the linear potential and one can compare the spectrum to that of open relativistic strings in flat space. In all cases the meson masses are of order the quark mass. On top of this spectrum of highly spinning strings, there are deeply bound mesons with  $J = 0, 1$  that are dual to the small fluctuations of the flavor brane worldvolume fields [7]. Their masses are of order  $\frac{m}{\sqrt{\lambda}}$  and they have been analyzed before at finite temperature [8–12] and non-vanishing magnetic field [13–15] or finite chemical potential [16]. For a review see [17]. Our studies complement these results for  $J = 0, 1$  supergravity mesons by analyzing the highly spinning mesons with semiclassical strings in AdS.

In the next section we start with a review of the meson properties at zero temperature. In section 3 we then analyze mesons and their dissociation at finite temperature. The results

are very similar to those obtained in [18] for the closely related Sakai-Sugimoto model [19]. In section 4 we study mesons in a background magnetic field and compare to results for the Zeeman splitting both in hydrogen and for a relativistic string in the appropriate limits. Finally, in section 5, we bring the two together and study the dissociation of mesons at finite temperature in the presence of a magnetic field.

## 2. Meson properties at zero temperature

Highly spinning mesons at zero temperature were first studied in [7]. The corresponding bulk configuration is a string with both of its ends on the flavor brane. For large angular momentum  $J \gg 1$ , the length of the string is much larger than  $l_s$  and it can be analyzed using the classical Nambu-Goto action in an AdS background. Writing the background AdS metric (setting the curvature radius to 1) as

$$ds^2 = -h(r)dt^2 + r^2 d\vec{x}^2 + \frac{dr^2}{h(r)} \quad (2.1)$$

with  $h(r) = r^2$  we are interested in stationary string configurations whose endpoints describe a circular orbit in the  $\vec{x}$  directions. Writing  $d\vec{x}^2 = d\rho^2 + \rho^2 d\theta^2$  we are hence looking for a string whose worldvolume is described by

$$\theta = \omega t, \quad r = r(\sigma), \quad \rho = \rho(\sigma). \quad (2.2)$$

The Nambu-Goto action for this ansatz becomes

$$S = -\frac{\sqrt{\lambda}}{2\pi} \int dt d\sigma \sqrt{(r'^2 + \rho'^2 r^2 h(r)) \left(1 - \frac{\omega^2 \rho^2 r^2}{h(r)}\right)} = -\frac{\sqrt{\lambda}}{2\pi} \int dt d\sigma \sqrt{(1 - \omega^2 \rho^2)(r'^2 + r^4 \rho'^2)} \quad (2.3)$$

where we used that in the units where the AdS curvature radius is one, the string tension is simply

$$\frac{1}{2\pi\alpha'} = \frac{\sqrt{\lambda}}{2\pi}. \quad (2.4)$$

The energy and angular momentum of the string follow immediately

$$J = \frac{\partial L}{\partial \omega} = \frac{\sqrt{\lambda}}{2\pi} \int d\sigma \omega \rho^2 \sqrt{\frac{r'^2 + r^4 \rho'^2}{1 - \omega^2 \rho^2}} \quad (2.5)$$

$$E = \omega \frac{\partial L}{\partial \omega} - L = \frac{\sqrt{\lambda}}{2\pi} \int d\sigma \sqrt{\frac{r'^2 + r^4 \rho'^2}{1 - \omega^2 \rho^2}}. \quad (2.6)$$

The equation of motion is straightforward. The Neumann boundary condition on  $\rho$  that follows from the variation of this Lagrangian is

$$0 = \pi_\rho^1 = \frac{\partial L}{\partial \rho'} = \frac{\sqrt{\lambda}}{2\pi} \frac{\rho' r^4}{\omega \rho} \sqrt{\frac{1 - \omega^2 \rho^2}{r'^2 + r^4 \rho'^2}} \quad (2.7)$$

which simply demands  $\rho' = 0$  at the end, that is the string ends on the flavor brane at a right angle at both ends. Since the configurations we are interested in are even under reflection around the string midpoint, one can alternatively specify a boundary condition each at the string midpoint and at a single endpoint.

To proceed, one can further fix the  $\sigma$  reparametrization invariance. Two convenient gauge choices seem to be either the  $\sigma = \rho$  or the  $\sigma = r$  static gauge. Both lead to large gradients which makes the numerics unstable. For the numerics we found that a very efficient choice is

$$\sigma = \rho + r \tag{2.8}$$

and hence  $\rho' + r' = 1$ . Numerically, we impose boundary conditions in the IR, demanding that a turnaround point exists at  $\rho = 0$ . That is, at  $\sigma = r_0$  we impose the boundary conditions

$$r(r_0) = r_0, \quad r'(r_0) = 0 \quad \Rightarrow \quad \rho(r_0) = 0, \quad \rho'(r_0) = 1. \tag{2.9}$$

For every choice of turnaround position  $r_0$  one then looks for the first  $r_m > r_0$  at which the UV boundary condition  $\rho'(r_m) = 0$  is satisfied. This way one avoids shooting and every numerical run will generate a valid solution for some mass  $m$  that is given in terms of  $r_m$  by

$$m = \frac{\sqrt{\lambda}}{2\pi} r_m. \tag{2.10}$$

With this numerical procedure we were able to reproduce the spectrum of mesons  $E(J)$  that was previously obtained in [7]. Our numerical results, together with the analytic limits we are about to discuss, are displayed in figure (2). We use the same gauge and numerical methods for our analysis in later sections.

As discussed in the introduction there are two regimes in which we expect to be able to compare the meson spectrum against analytic formulas. For large  $J \gg \sqrt{\lambda}$  we are in a Coulombic regime where the potential  $V(r) = -c_1/r$  with  $c_1$  given in eq.(1.1). The system is non-relativistic in this regime. The standard non-relativistic boundstate spectrum in a Coulomb potential is given by (including the rest-mass  $2m$  of the two quarks)

$$E(J)/m = 2 - \frac{c_1^2}{2J^2} \frac{m^*}{m} = 2 - \frac{4\pi^4}{\Gamma(\frac{1}{4})^8} \frac{\lambda}{J^2} \tag{2.11}$$

where we used that the reduced mass is  $m^* = \frac{m_1 m_2}{m_1 + m_2} = \frac{m}{2}$  for two equal mass particles. The other tractable region is  $1 \ll J \ll \sqrt{\lambda}$  in which we expect standard Regge behavior

$$E^2 = 2\pi\tau_{eff} J \tag{2.12}$$

where the effective tension is given by eq.(1.2) so that

$$E/m = 2\pi \frac{\sqrt{J}}{\lambda^{1/4}}. \tag{2.13}$$

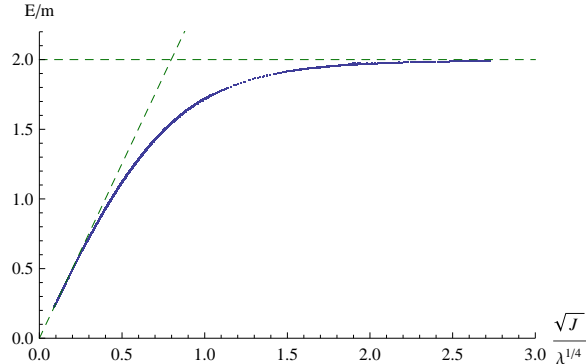


**Figure 2:** Meson energy  $E/m$  as a function of  $\sqrt{J}/\lambda^{1/4}$ .  $E/m = 2$  is the rest mass of the quarks, so bound states only exist for  $E/m \leq 2$ . Also indicated are the two limiting case of a pure Coulomb potential which is a good approximation for  $J \gg \sqrt{\lambda}$  and Regge behavior for  $1 \ll J \ll \sqrt{\lambda}$ .

### 3. Meson dissociation at finite temperature

In this section we study how the spectrum of highly spinning mesons is modified at finite temperature. In particular, we study the dissociation of the most weakly bound mesons as the temperature is raised. The disappearance of these bound states leads to a critical  $J_{crit}(m/T)$ , where mesons with  $J > J_{crit}$  become unstable. The mesons of flavored  $\mathcal{N} = 4$  have been proposed as a model for charmonium boundstates at finite temperature e.g. in reference [20] where their dissociation as a function of linear velocity has been analyzed. The study of meson dissociation is then potentially relevant for studies at heavy ion colliders. Meson dissociation in the closely related Sakai-Sugimoto model has been analyzed in [18] with qualitatively similar results.

In the numerical analysis, the only difference with the zero temperature case is that in the action we need to set  $h(r) = r^2 - \frac{r_h^4}{r^2}$  with  $r_h = \pi T$  instead of the  $h(r) = r^2$  we had before. In interpreting the result, some care has to be taken in what one means by mass. As discussed in [21] at finite temperature (and the same comment will later apply to finite magnetic field) there are several notions of mass which all coincided in the  $B = T = 0$  case. One is the mass parameter that appears in the Lagrangian,  $m_L$ . This is related to the position  $r_m$  at which the flavor brane ends in a non-trivial fashion as first discussed in [8]. One needs to know the exact embedding of the brane, which changes both in response to the temperature and the magnetic field. These embeddings have been obtained in [15, 22] A physical definition of mass that is directly related to  $r_m$  is the rest mass of a quasi-particle, which was denoted  $M_{rest}$  in [21]. This is simply the energy that one has to pay to create a flavored quasi-particle and hence just given by the length of the string stretching from the horizon to the flavor brane times the tension. For our purposes, we will continue referring to  $m = \frac{\sqrt{\lambda}}{2\pi} r_m$  as “the mass”. In the language of [21] this is  $M_{rest} + \Delta m$ , latter being the thermal mass shift,  $\Delta m = \frac{\sqrt{\lambda}}{2} T$ . All other notions of mass can simply be determined in terms of  $m$ , for details see [21]. With

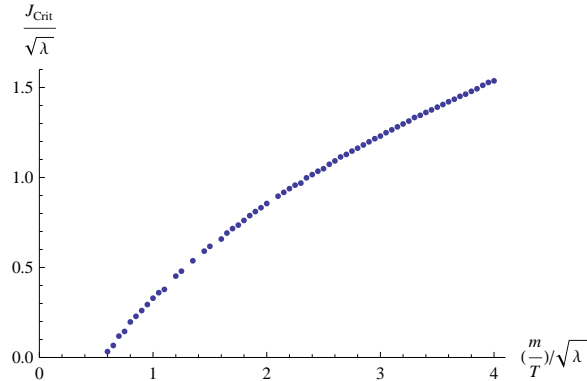


**Figure 3:**  $J_{crit}$  as a function of  $\frac{m}{T}$ .

this definition of mass the minimal mass is  $M_{rest} = 0$  and hence  $m = \Delta m = \frac{\sqrt{\lambda}}{2}T$ . This is the point where the brane touches the horizon. This minimal value of  $m$  appears in several of our plots.

Figure (3) displays our result for the critical angular momentum as a function of  $m/T$ . As in the zero temperature case, one might be tempted to give an interpretation of  $J_{crit}(m/T)$  using a field theory model of two massive quarks moving in an effective potential. However, such an interpretation is only sensible in the non-relativistic regime. At finite temperature, due to screening, the quark/anti-quark potential becomes short range and the non-relativistic regime gets removed first. For relativistic bound-states, a significant fraction of the angular momentum and energy gets carried by the flux tube for which we only have a 5d description. Qualitatively, the fact that  $J_{crit}$  drops as the temperature rises is consistent with an interpretation of bound states melting.

Last but not least note that our semiclassical string configurations only probe the short distance part of the quark/anti-quark potential that scales as  $\sqrt{\lambda}$ . As argued in [23] there will be an exponential tail on top of this with an order one coefficient. All we can say with confidence is that for angular momenta above  $J_{crit}$  mesons with binding energies of order  $\sqrt{\lambda}$  do not exist. There might be bound states with order one binding energies which would be represented by spinning strings stabilized by quantum corrections.

## 4. Zeeman effect

### 4.1 General Considerations

In this section we study the effect of a background magnetic field on the meson spectrum. At zero magnetic field rotational symmetry ensures that the energy of the mesons only depends on the magnitude  $J$  of the angular momentum and not its direction. As usual, the magnetic field breaks this degeneracy and introduces additional dependence of the meson masses on the scalar product  $\vec{J} \cdot \vec{B} = m_j B$ . With this definition of  $m_j$ , it takes values between  $-J$  and  $+J$  as

usual. Since we are working in the limit of large  $J$  we do not see the quantization of  $m_j$ . For a generic orientation of  $\vec{J}$  and  $\vec{B}$ , the orbits of the quark/antiquark pair will no longer be circular and our ansatz for the bulk string configuration is too simple-minded. However, the same ansatz eq.(2.2) can still capture the two extreme cases of  $m_j = \pm J$ , that is the magnetic field is either completely aligned or anti-aligned with the angular momentum. These two extreme cases are sufficient to analyze the splitting in the magnetic field background. For small  $B$ , one can linearize the energies in  $\vec{J} \cdot \vec{B}$  and find the standard behavior

$$\Delta E = a(J) m_j B. \tag{4.1}$$

Calculating the energy splitting for  $m_j = \pm J$  is completely sufficient to determine  $a(J)$ . When non-linearities in  $B$  become important, we can still exactly trace the two extreme levels. Values of  $-J < m_j < J$  are expected to lie in between. They need no longer be equally spaced.

There are actually two cases we will discuss and need to distinguish: quark/anti-quark pairs with equal opposite charges or with equal charges. Of course they will always be oppositely charged under the gauged  $SU(N)$  symmetry. For a single flavor brane, there is just one global  $U(1)$  gauge field living on the flavor brane, baryon number. The quark and the anti-quark carry equal and opposite charge under this global symmetry. Since quark and anti-quark have the same mass, the orbital magnetic moment of the two actually cancels and, like in positronium, the linear Zeeman splitting does not affect states with different values of  $m_j$ . To see any non-trivial linear Zeeman splitting we hence also study the case of equally charged string endpoints. One way to achieve this is to look at 2 flavor branes A and B, so that the global flavor symmetry is  $U(1)_A \times U(1)_B$  and then turn on equal opposite fields in the two  $U(1)$  factors. While the AA and BB strings will, like before, have equal opposite charges under this field, the AB or BA strings will have equal charges. For simplicity, we only look at 2 flavors of equal mass, but obviously our method can be extended to the case of two unequal mass flavors. The corresponding field theory and gravity configurations are sketched and contrasted in figure (4).

In the case of equal opposite charges, there is no linear Zeeman splitting since the magnetic moments of the two particles cancel. There can however be a correction to the energies quadratic in  $B$ . Since the only two configurations we can realize in the supergravity correspond to  $\vec{J} \cdot \vec{B} = \pm JB$ , in this case there will be no splitting and the two configurations will have identical energies. It is indeed easy to see both in the field theory and the supergravity that in the case of equal opposite charges, there is a  $Z_2$  symmetry that takes  $\vec{J} \rightarrow -\vec{J}$  and at the same time exchanges the endpoints of the string. This symmetry operation takes one configuration into a different one with identical energy but opposite sign of  $\vec{J} \cdot \vec{B}$ . For the case of  $1 \ll J \ll \sqrt{\lambda}$  we can compare our supergravity analysis with the study of a Nambu-Goto string in a background magnetic field. This was analyzed in the classic paper [24] where it was found that in the case of equal opposite charges there is no change in the string spectrum whatsoever, even though the actual string configuration changes: the string starts to fold back onto itself as indicated in the left of figure (4). So for  $J \ll \sqrt{\lambda}$  the energy shift as a



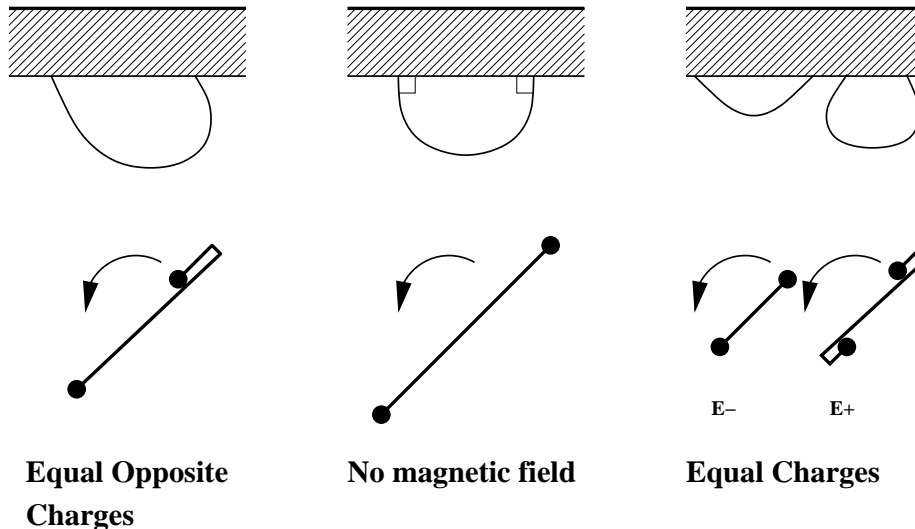


**Figure 4:** Sketch of supergravity and field theory configurations for the cases of equal opposite and equal charges of the string endpoints. In the field theory picture the circles indicate the position of quark and anti-quark, whereas the thick lines are the flux-tubes. In the case of equal opposite charges there is no net magnetic moment since the contributions from quark and anti-quark cancel. In this case there is a second configuration with the same energy that is the mirror image of the one depicted. In the case of equal charges the two contributions to the orbital angular momentum add up. There are two configurations with energies  $E_{\pm} = E \pm \Delta E$ .

function of  $B^2$  has to vanish. For  $J \gg \sqrt{\lambda}$  one expects a non-trivial shift in the energy, even though there will not be any splitting between the two configurations with opposite  $\vec{J} \cdot \vec{B}$ .

In the case of equal charges, we should see the familiar pattern of Zeeman splitting with a shift proportional to  $\vec{J} \cdot \vec{B}$  so that for any given  $J$  and  $B$  we will find two configurations with circular orbit and energies  $E(B=0) \pm \Delta E$  with  $\Delta E$  of the form indicated in eq. (4.1). At  $J \gg \sqrt{\lambda}$  we can compare our results to an analysis of a purely Coulombic Hydrogen-like system. In this case we expect

$$\frac{\Delta E}{m} = \frac{\mu_B J B}{m} = \frac{B}{2m^2} J \quad (4.2)$$

where  $\mu_B = \frac{1}{2m}$  is the standard Bohr magneton for particles of unit charge.  $\frac{E}{m}$  and  $\frac{B}{m^2}$  are the dimensionless quantities measuring the energy and the magnetic field in units of the quark mass. Since our theory is conformal, the physics can only depend on these ratios and not on  $E$ ,  $B$  and  $m$  individually. For  $1 \ll J \ll \sqrt{\lambda}$  one can once more compare to the spectrum of a Nambu-Goto string with tension  $\tau_{eff}$  in a background magnetic field. For equal charges it was found in [24] that for large  $J$  one has

$$E^2 = 2\pi\tau_{eff}(1 - \epsilon)J \quad (4.3)$$

where

$$\epsilon = \frac{2}{\pi} \arctan\left(\frac{B}{\tau_{eff}}\right) = \frac{2}{\pi} \frac{B}{\tau_{eff}} + \mathcal{O}(B^3) \quad (4.4)$$

so that to linear order in  $B$  we expect for the change in energy

$$\frac{\Delta E}{m} = 2 \frac{1}{\sqrt{2\pi\tau_{eff}}} \sqrt{J} \frac{B}{m} = \frac{B}{\pi m^2} \lambda^{1/4} \sqrt{J}. \quad (4.5)$$

## 4.2 Supergravity analysis

The presence of a constant magnetic field in the  $(\rho, \theta)$  plane with  $F = B dx \wedge dy = B \rho dr \wedge d\theta$  only modifies the string action via the additional boundary terms.

$$\Delta S = \int d\tau A \Big|_{\sigma^+} \mp \int d\tau A \Big|_{\sigma^-} \quad (4.6)$$

where  $\sigma^\pm$  refers to the right and left boundary (which in our gauge choice is not simply at  $\sigma = \pi, 0$ ) and the upper (lower) sign corresponds to the case of equal opposite (equal) charges. Choosing  $A_\rho = 0$  gauge we have as the only non-vanishing component

$$A_\theta = B \frac{\rho^2}{2} \quad (4.7)$$

and the action (4.6) becomes (noting that  $\frac{d\theta}{dt} = \omega$ )

$$\Delta S = B \int d\tau \frac{\rho^2 \omega}{2} \Big|_{\sigma^+} \mp B \int d\tau \frac{\rho^2 \omega}{2} \Big|_{\sigma^-}. \quad (4.8)$$

This leads to two basic changes when compared to the analysis of section 2. First, the boundary condition gets modified to

$$\pi_\rho^1 = -F_{\rho\theta} \dot{\theta} = -B\rho\omega. \quad (4.9)$$

Second, the boundary terms in the action give an additional contribution to  $J = \frac{\partial L}{\partial \omega}$

$$\Delta J = B \frac{\rho^2}{2} \Big|_{\sigma^+} \mp B \frac{\rho^2}{2} \Big|_{\sigma^-} \quad (4.10)$$

The corresponding contribution to the energy  $E = \omega \frac{\partial L}{\partial \omega} - L$  cancels since the boundary action is linear in  $\omega$ . A similar discussion appears in [25] where mesons in a non-commutative theory were analyzed which corresponds to a gravity solution with non-trivial background H-flux.

For the case of two equal charges, the configurations are once again symmetric under reflection around the midpoint and one can then simply perform the numerical analysis along the same lines as in the zero temperature, zero B-field case. For every choice of turnaround point  $r_0$  one generates a string configuration that solves the equation of motion. For every choice of  $r_m$  one then can subsequently read off a  $B$  that allows one to have the boundary condition satisfied at that value of  $r_m$ . The change in angular momentum in this case is given

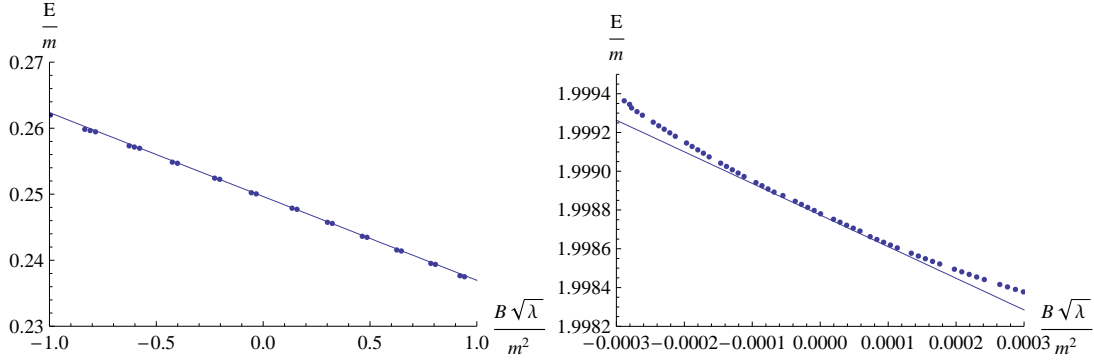


**Figure 5:** Numerical results for  $E/m$  as a function of  $B/m^2$  for  $J/\sqrt{\lambda} = 0.00159$  and for  $J/\sqrt{\lambda} = 3.34$  together with analytic results from the Regge and Coulomb regimes respectively in the case of equal charges.

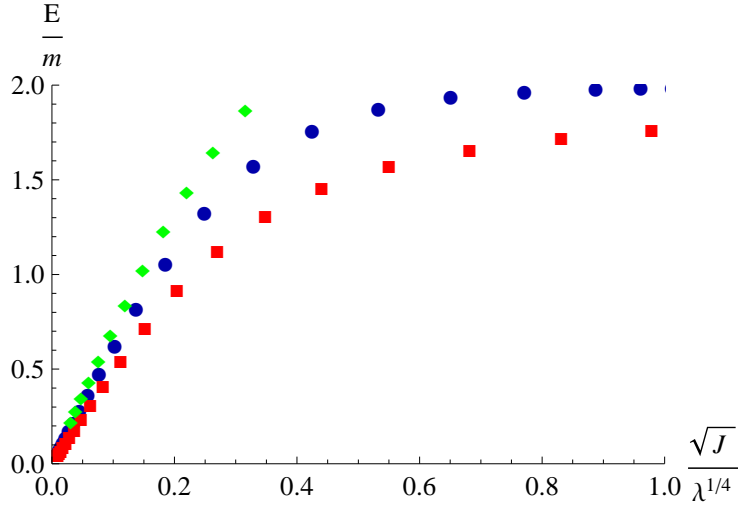


**Figure 6:**  $E/m$  as a function of  $J$  for  $B\sqrt{\lambda}/m^2 = 0.1$  (blue squares),  $B = 0$  (red circles) and  $B\sqrt{\lambda}/m^2 = -0.1$  (green diamonds).

by  $\Delta J = B\rho^2|_{\sigma+}$ . We present our results for the meson spectrum in this case as a function of  $B/m^2$  together with a comparison to the analytic results for the  $1 \ll J \ll \sqrt{\lambda}$  and  $J \gg \sqrt{\lambda}$  regimes in figure (5).

In figure (6) we show the energies for  $\frac{B\sqrt{\lambda}}{m^2} = \pm 0.1$  as a function of  $J$ . In the left panel of figure (7) we also show one example of a calculation performed at an intermediate  $J$  for arbitrary  $B$  exhibiting interesting non-linear effects in  $B$ .

In the case of equal opposite charges one has to deal with the additional complication that the configuration is no longer symmetric with respect to reflection around the string midpoint. In our numerical scheme this means we can no longer assume that the turnaround

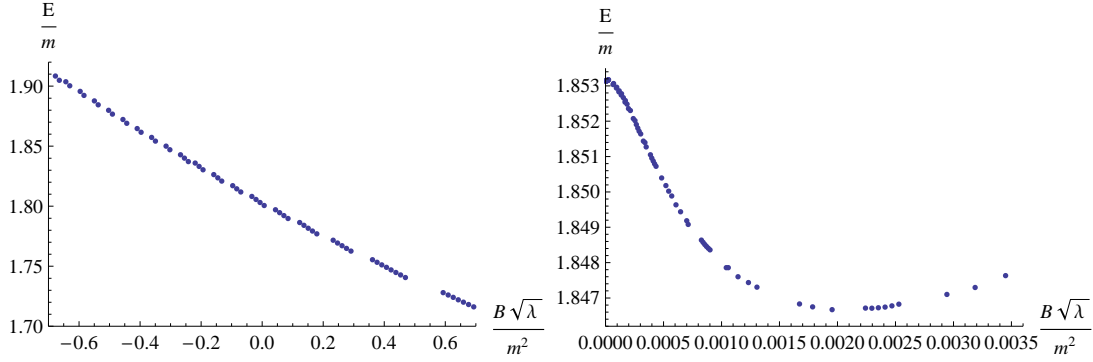


**Figure 7:** Left panel: Meson spectrum  $E/m$  as a function of  $B/m^2$  for  $J/\sqrt{\lambda} = 0.207$  for equal charges. Right Panel: Meson spectrum  $E/m$  as a function of  $B/m^2$  for  $J/\sqrt{\lambda} = 0.255$  for equal opposite charges. Note that for equal opposite charges the linear Zeeman effect does not contribute since the meson has no net magnetic moment, the shift starts at quadratic order in  $B$ .

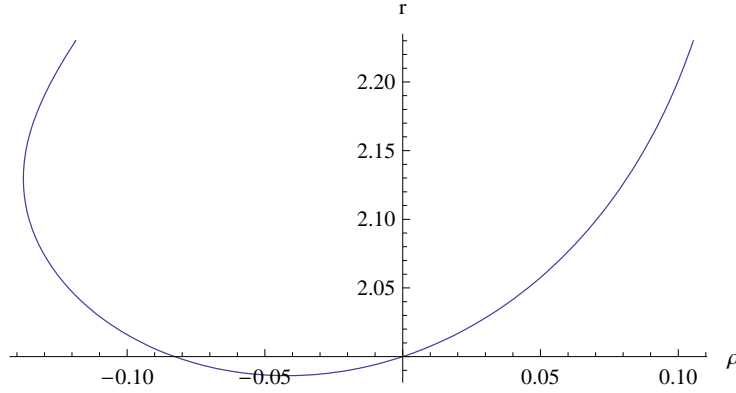


**Figure 8:** String profile  $r(\rho)$  for the case of equal opposite charges with  $\frac{J}{\sqrt{\lambda}} = 0.126$  and  $\frac{B}{m^2} = \frac{3.64}{\sqrt{\lambda}}$ .

point is at  $\rho = 0$ . We therefore must chose both  $r_0$  and  $r'_0$  at  $\rho = 0$ . That is at  $\sigma_0 = r_0$  we impose the boundary conditions

$$r(\sigma_0) = r_0, \quad r'(\sigma_0) = r'_0. \quad (4.11)$$

For every  $r_m$  one can once more find a  $B$  that makes the UV boundary condition true at either end of the string. But only for special values of  $r_m$  will one get the boundary condition to be true with the *same*  $B$  at both ends. We therefore use a shooting algorithm where, for a given string solution, we step through possible values of the mass to find the special  $r_m$ 's for which the asymmetric boundary conditions are satisfied. We present our results for the meson spectrum in this case in the right panel of figure (7). A typical string configuration for this case of equal opposite charges is displayed in figure (8)

### 4.3 $J \ll \sqrt{\lambda}$ , equal charges

An analytic solution to the equations of motion can be found in the case  $\omega \rightarrow \infty$ , following a procedure similar to the one in [7]. We will see that this case corresponds to  $J \ll \sqrt{\lambda}$ . To simplify the equations, we use the coordinates  $\tilde{z} = \omega z = \omega/r$ ,  $\tilde{\rho} = \omega\rho$  and the gauge  $\tilde{\rho} = \sigma$ . The equation of motion for  $\tilde{z}$  is then

$$\frac{\tilde{z}''}{1 + \tilde{z}'^2} + \frac{2}{\tilde{z}} - \frac{\tilde{\rho}\tilde{z}'}{1 - \tilde{\rho}^2} = 0 \quad (4.12)$$

We can substitute the ansatz  $\tilde{z} = \omega z_{D7} + \frac{1}{\omega z_{D7}} f(\tilde{\rho})$  into (4.12), where  $z_{D7}$  is the position of the D7 brane. Keeping only terms of order  $1/\omega z_{D7}$  we get an equation for  $f$ ,

$$f'' - 2 - \frac{\tilde{\rho}f'}{1 - \tilde{\rho}^2} = 0 \quad (4.13)$$

From the boundary conditions for  $\tilde{z}$ , we find the boundary conditions  $f(0) = 0$  and  $f'(0) = 0$ . Then, solving for  $f$ ,

$$f(\tilde{\rho}) = \frac{1}{2}(\tilde{\rho}^2 + \arcsin^2(\tilde{\rho})). \quad (4.14)$$

At the boundary  $\rho$  must satisfy  $\pi_\rho^1 = \frac{\partial L}{\partial \rho} = -\rho B\omega$ . So,

$$\frac{\sqrt{\lambda}}{2\pi} \frac{1}{\tilde{z}^2} \sqrt{\frac{1 - \tilde{\rho}^2}{1 + \tilde{z}'^2}} = -\tilde{\rho}B \quad (4.15)$$

Substituting the equation for  $\tilde{z}$ , we see that the critical value of  $\tilde{\rho}$  at the boundary must satisfy, for small  $B$ ,

$$\tilde{\rho}_C = \frac{\sqrt{\lambda}/2\pi}{\sqrt{\lambda/4\pi^2 + B^2 z_{D7}^4}} \approx 1 - \frac{B^2 z_{D7}^4 \pi^2}{\lambda}. \quad (4.16)$$

Putting all of this into the equations for  $E$  and  $J$ , including the endpoint contribution to  $J$  (4.10), using that  $z_{D7} = \frac{\sqrt{\lambda}}{2m\pi}$ , and keeping terms linear in  $B$ , we find that

$$E = \frac{\sqrt{\lambda}}{2z_{D7}^2\omega} - \frac{2B}{\omega} \quad (4.17)$$

$$J = \frac{\sqrt{\lambda}}{4z_{D7}^2\omega^2} - \frac{B}{\omega^2} \quad (4.18)$$

Since  $\omega$  is large,  $J \ll \sqrt{\lambda}$ , as we expected. Solving for  $E$  in terms of  $J$ , using (2.10) and again keeping only terms linear in  $B$ ,

$$\frac{E}{m} = \frac{2\pi\sqrt{J}}{\lambda^{1/4}} - \frac{\sqrt{J}\lambda^{1/4}}{\pi} \frac{B}{m^2}. \quad (4.19)$$

To find the energy of the upper branch, we must integrate from  $\rho_C$  to  $\rho = 1$ , and then from  $\rho = 1$  back to  $\rho = 0$  to take into account the shape of the string configurations as we see in figure (4). We find the energy of this branch to be,

$$\frac{E}{m} = \frac{2\pi\sqrt{J}}{\lambda^{1/4}} + \frac{\sqrt{J}\lambda^{1/4}}{\pi} \frac{B}{m^2}. \quad (4.20)$$

So the splitting is  $\Delta E/m = \sqrt{J}\lambda^{1/4}B/m^2\pi$ , which is consistent with what was obtained in (4.5).

#### 4.4 $J \ll \sqrt{\lambda}$ , opposite charges

For the case of equal and opposite charges, the boundary condition is different for the left and right ends of the string.

$$\pi_1^\rho|_\pm = \pm\rho B\omega \quad (4.21)$$

As we can see from the string profile in figure (4), on one side of the string, we must again integrate from  $\rho_C$  to  $\rho = 1$  to  $\rho = 0$ , as in the upper branch of the equal charge case. The other side of the string is integrated as in the lower branch of the equal charges case. Following the same method as before, we obtain,

$$E = \frac{\pi}{z_{D7}^2\omega} \quad (4.22)$$

$$J = \frac{\pi}{2z_{D7}^2\omega^2} \quad (4.23)$$

so

$$E/m = \frac{2\pi\sqrt{J}}{\lambda^{1/4}} \quad (4.24)$$

which does not depend linearly on  $B$ . In this case, exact evaluation of the integrals of the small  $J$  solution without using the additional approximation (4.16) shows that  $E$  does not depend on  $B$ . To see what this means, consider writing  $E^2$  as a power series in  $J$  with functional prefactors  $C_i(B)$ ,

$$(E/m)^2 = \sum_i C_i(B)J^i. \quad (4.25)$$

The result above is simply the statement that  $C_1$  is the constant  $4\pi^2/\sqrt{\lambda}$ . This is in perfect agreement with the result of [24] that for a field theory Nambu-Goto flux tube with equal opposite charges the energy is completely independent of  $B$ .

## 5. Meson dissociation in the presence of magnetic fields

Last but not least, we want to put together the two cases we studied in the last two sections and study the strings when both temperature and external magnetic field are turned on. There are of course now many different parameters to tune: the temperature, the mass, the magnetic field, and the angular momentum. The main point we want to make here is that one can map out the properties of the strings as a function of all those control parameters using our technique. One particularly interesting quantity we calculate is once more the critical angular momentum  $J_{crit}(m/T, B/m^2)$  beyond which the mesons dissociate. In figure (9) we show  $J_{crit}$  as a function of  $m/T$  for  $B = \pm 0.157\sqrt{\lambda}T^2$ . As expected, the magnetic field increases the binding energy of at least one state and hence increases  $J_{crit}$  when compared to the zero temperature cases.

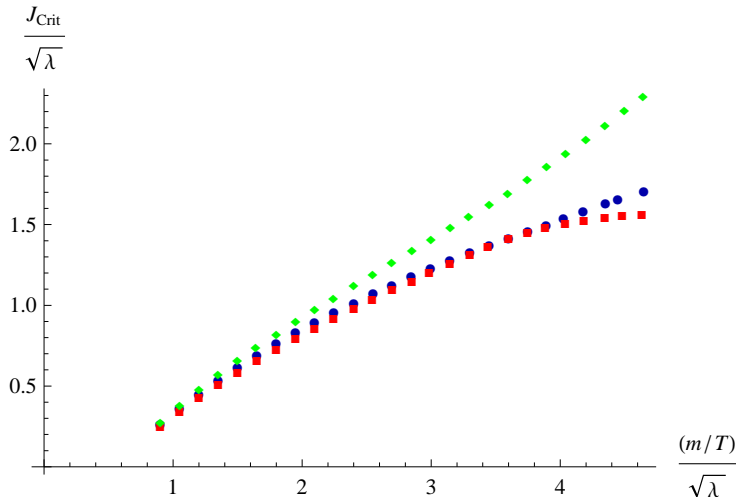


**Figure 9:**  $J_{\text{crit}}$  as a function of  $m/T$  for  $\frac{B}{\sqrt{\lambda}T^2} = -0.157$  (green diamonds), 0 (blue circles) and  $+0.157$  (red squares).

## Acknowledgments

We would like to thank M. Baker and in particular C. Herzog for useful discussions. This work was supported in part by the U.S. Department of Energy under Grant No. DE-FG02-96ER40956.

## References

- [1] J. M. Maldacena, *The large  $N$  limit of superconformal field theories and supergravity*, *Adv. Theor. Math. Phys.* **2** (1998) 231–252, [[hep-th/9711200](#)].
- [2] E. Witten, *Anti-de Sitter space and holography*, *Adv. Theor. Math. Phys.* **2** (1998) 253–291, [[hep-th/9802150](#)].
- [3] S. S. Gubser, I. R. Klebanov, and A. M. Polyakov, *Gauge theory correlators from non-critical string theory*, *Phys. Lett.* **B428** (1998) 105–114, [[hep-th/9802109](#)].
- [4] J. M. Maldacena, *Wilson loops in large  $N$  field theories*, *Phys. Rev. Lett.* **80** (1998) 4859–4862, [[hep-th/9803002](#)].
- [5] S.-J. Rey and J.-T. Yee, *Macroscopic strings as heavy quarks in large  $N$  gauge theory and anti-de Sitter supergravity*, *Eur. Phys. J.* **C22** (2001) 379–394, [[hep-th/9803001](#)].
- [6] A. Karch and E. Katz, *Adding flavor to AdS/CFT*, *JHEP* **06** (2002) 043, [[hep-th/0205236](#)].
- [7] M. Kruczenski, D. Mateos, R. C. Myers, and D. J. Winters, *Meson spectroscopy in AdS/CFT with flavour*, *JHEP* **07** (2003) 049, [[hep-th/0304032](#)].
- [8] J. Babington, J. Erdmenger, N. J. Evans, Z. Guralnik, and I. Kirsch, *Chiral symmetry breaking and pions in non-supersymmetric gauge/gravity duals*, *Phys. Rev.* **D69** (2004) 066007, [[hep-th/0306018](#)].

- [9] T. Albash, V. Filev, C. V. Johnson, and A. Kundu, *A topology-changing phase transition and the dynamics of flavour*, [hep-th/0605088](#).
- [10] D. Mateos, R. C. Myers, and R. M. Thomson, *Thermodynamics of the brane*, *JHEP* **05** (2007) 067, [[hep-th/0701132](#)].
- [11] C. Hoyos, K. Landsteiner, and S. Montero, *Holographic meson melting*, *JHEP* **04** (2007) 031, [[hep-th/0612169](#)].
- [12] R. C. Myers, A. O. Starinets, and R. M. Thomson, *Holographic spectral functions and diffusion constants for fundamental matter*, [arXiv:0706.0162](#) [[hep-th](#)].
- [13] V. G. Filev, C. V. Johnson, R. C. Rashkov, and K. S. Viswanathan, *Flavoured large  $n$  gauge theory in an external magnetic field*, [hep-th/0701001](#).
- [14] V. G. Filev, *Criticality, scaling and chiral symmetry breaking in external magnetic field*, [arXiv:0706.3811](#) [[hep-th](#)].
- [15] J. Erdmenger, R. Meyer, and J. P. Shock, *Ads/cft with flavour in electric and magnetic kalb-ramond fields*, *JHEP* **12** (2007) 091, [[arXiv:0709.1551](#) [[hep-th](#)]].
- [16] J. Erdmenger, M. Kaminski, and F. Rust, *Holographic vector mesons from spectral functions at finite baryon or isospin density*, [arXiv:0710.0334](#) [[hep-th](#)].
- [17] J. Erdmenger, N. Evans, I. Kirsch, and E. Threlfall, *Mesons in gauge/gravity duals - a review*, [arXiv:0711.4467](#) [[hep-th](#)].
- [18] K. Peeters, J. Sonnenschein, and M. Zamaklar, *Holographic melting and related properties of mesons in a quark gluon plasma*, *Phys. Rev.* **D74** (2006) 106008, [[hep-th/0606195](#)].
- [19] T. Sakai and S. Sugimoto, *Low energy hadron physics in holographic QCD*, *Prog. Theor. Phys.* **113** (2005) 843–882, [[hep-th/0412141](#)].
- [20] H. Liu, K. Rajagopal, and U. A. Wiedemann, *An AdS/CFT calculation of screening in a hot wind*, *Phys. Rev. Lett.* **98** (2007) 182301, [[hep-ph/0607062](#)].
- [21] C. P. Herzog, A. Karch, P. Kovtun, C. Kozcaz, and L. G. Yaffe, *Energy loss of a heavy quark moving through  $n = 4$  supersymmetric yang-mills plasma*, *JHEP* **07** (2006) 013, [[hep-th/0605158](#)].
- [22] T. Albash, V. G. Filev, C. V. Johnson, and A. Kundu, *Quarks in an External Electric Field in Finite Temperature Large  $N$  Gauge Theory*, [arXiv:0709.1554](#) [[hep-th](#)].
- [23] D. Bak, A. Karch, and L. G. Yaffe, *Debye screening in strongly coupled  $n=4$  supersymmetric yang-mills plasma*, *JHEP* **08** (2007) 049, [[arXiv:0705.0994](#) [[hep-th](#)]].
- [24] A. Abouelsaood, J. Callan, Curtis G., C. R. Nappi, and S. A. Yost, *Open strings in background gauge fields*, *Nucl. Phys.* **B280** (1987) 599.
- [25] D. Arean, A. Paredes, and A. V. Ramallo, *Adding flavor to the gravity dual of non-commutative gauge theories*, *JHEP* **08** (2005) 017, [[hep-th/0505181](#)].